THE APPLICATION OF PIXEL BASED IMAGING TO SYNTHETIC APERTURE SONAR

R McHugh, S Shaw, N Taylor

Dept. Computing and Electrical Engineering, Heriot-Watt University, Edinburgh.

ABSTRACT

Synthetic aperture techniques are commonly applied in Radar processing enabling images to be produced with high, range independent resolution and are now widely proposed for application in Sonar. This paper presents application of Pixel Based imaging to synthetic aperture sonar, a technique successfully applied in forward looking sonar imaging. Four processing schemes are described showing the grating lobe suppression achieved with each scheme. Results from both simulation and test tank experiments are shown.

1. INTRODUCTION

Applied commonly in radar, synthetic aperture (SA) techniques have become widely discussed for application in sonar [1][2][3].

Synthetic aperture can be compared directly to side scan sonar in terms of vertical and range geometry. Figure 1 shows the azimuthal geometry normally considered where a real aperture of horizontal dimension *d* traverses a linear track. The length of track required to form a synthetic aperture for a particular slant range is equivalent to the conventional resolution of the real aperture at that distance, or distance the sonar platform travels during the time that a point to be resolved remains in the real aperture beam. The transducer acts both as transmitter and receiver resulting in a two way path length. This gives theoretical resolution of $d/2$ which is independent of frequency and slant range [4]5][6]. Spatial sampling in synthetic aperture as described by the pulse repetition frequency (PRF) is required to lie between two limits [4][5]. The lower limit is that to enable the sea bed to be continuously covered by the synthesised beams and the upper limit is that to ensure no range ambiguity due to multiple pulses being present at the receiver over the collection interval. Spatial sampling at $d/2$ theoretically enables reduction of grating lobes by the response of the real aperture [5]. Data collected over the synthetic aperture position should be coherent, although non-coherent suboptimal processing schemes have been proposed [8][9]. As the returns at each synthetic element are not derived from a common transmission a high degree of phase stability is required [9]. Phase instability resulting from inconsistencies in the

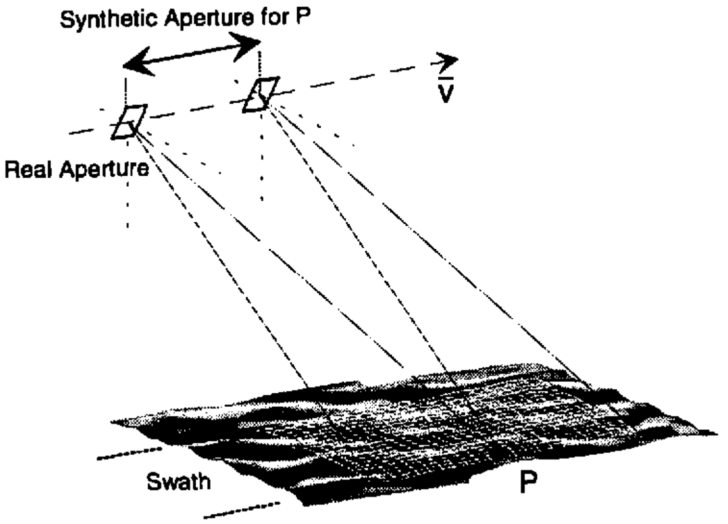

Figure 1 *Synthetic aperture geometry.*

transmission medium are shown generally not to be as significant over the time intervals in question [10][11]. Coherency is also impaired by deviations from a perfectly linear track [9], giving rise to the requirement for motion compensation [12][13]. SA processing is essentially a two dimensional replica correlation, or matched filtering operation [8][14] in which the set of sampled returns from a track sampled at a defined pulse repetition frequency (PRF) is correlated with the theoretical replica set created from knowledge of the transmitted pulse and data collection system.

The digital focused beamforming algorithm (DFB) was initially conceived for forward looking pixel based imaging and the flexibility of the technique has been successfully demonstrated using a prototype system [15]. DFB has developed taking into consideration the architecture and structure of modern digital signal processors employing vector and matrix based operations. The technique has proved flexible in application a number of other modes of sonar imaging, including sidescan and sidescan swath bathymetry. This paper overviews DFB and its application to synthetic aperture processing.

2. DIGITAL FOCUSED BEAMFORMER ALGORITHM

The exact steering delays in a digital beamformer are approximated by integer increments of the input sampling rate $T_s = f_s^{-1}$. If sampling is restricted to the Nyquist rate, these approximations are not acceptable for delay sum beamforming. Sampling rates of the order of ten times Nyquist are generally required [16]. Interpolation can be applied to artificially increase the sampling rate using FIR and IIR based interpolation methods[17][18]. Beamforming can also be achieved using a sampling regime based on the signal bandwidth, or bandpass sampling [18][19] through description of a signal by its complex components. Bandpass sampling techniques are considered to increase computational efficiency by reducing data rates and storage requirements. These methods however generally impose a greater requirement for analogue signal conditioning prior to sampling. For a particular carrier frequency f_c, there also exists certain sampling frequencies where $f_s<f_c$, that can be used to effectively sample an alias of f_c. This is referred to as Nyquist subsampling.

DFB can be considered as a true time delay digital beamformer. Application of a phase interpolation technique enables an image quality to be obtained from data sampled at Nyquist which is equivalent to that obtained from highly over sampled data[15]. DFB however is not restricted to a particular sampling scheme, lowpass sampling at Nyquist and Nyquist sub-sampling having been demonstrated in simulation and using the prototype system.

A representation of the narrow band digital focused beamforming algorithm is shown in Figure 2. The algorithm can be subdivided into a set of individual operations, delay generation, data acquisition and filtering, phase shifting and summation followed by pixel power calculation.

APPLICATION OF PIXEL BASED IMAGING TO SYNTHETIC APERTURE SONAR

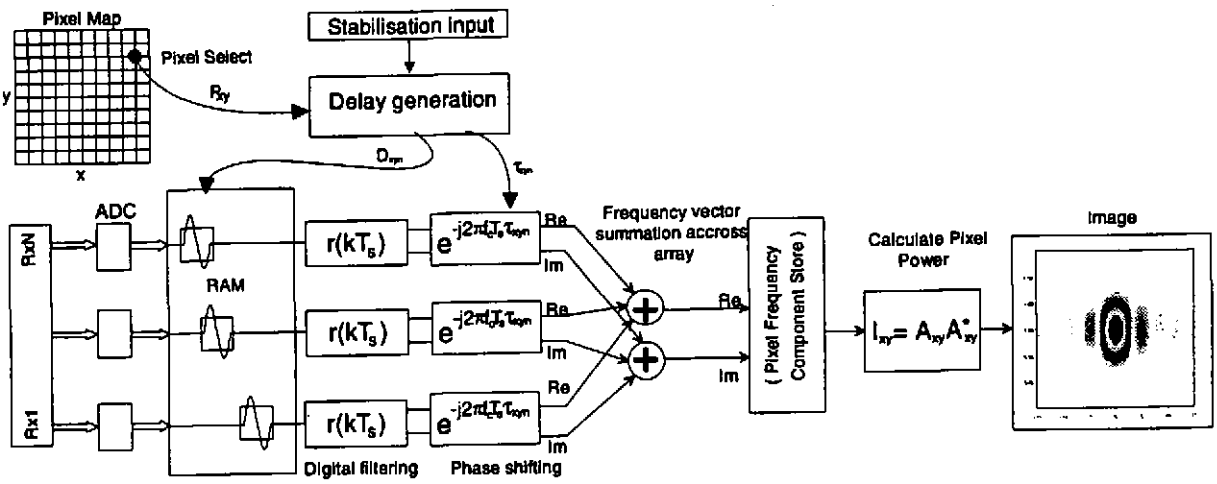

Figure 2 : *Diagrammatic representation of the Narrowband Digital Focused Beamforming algorithm*

The power of image pixel I_{xy} can be stated as

$$I_{xy} = \left| \sum_{n=1}^{N_e} a_n s_n (kT_s - D_{xyn}T_s)\exp(-j2\pi f_c T_s \tau_{xyn}) \right|^2 \quad (1)$$

where x and y are two dimensional image co-ordinates. $s_n(kT_s) = e_n(kT_s) \otimes r(kT_s)$ represents the correlation of the returned echo signal $e_n(kT_s)$, sampled at T_s, with a general filter function $r(kT_s)$ which can be a matched filter. a_n is the aperture shading function. D_{xyn} and τ_{xyn} are values derived from a calculated true time delay. D_{xyn} forms the basis of the mapping operation and is used to index complex spectral values $\alpha_{xyn} = a_{xyn} + jb_{xyn}$ from the correlation filter output. τ_{xyn} is used to fine phase shift the complex data by $\phi_{xyn} = 2\pi f_c T_s \tau_{xyn}$ rads using (2). The phase shift is equivalent to a time shift and used to align the measure of acoustic return exactly with the spatial point. Equation (2) can be expanded into trigonometric functions to give (3) which is a complex multiplication.

$$\alpha'_{xyn} = \alpha_{xyn} e^{j\phi_{xyn}} \quad (2)$$

$$\alpha'_{xyn} = (a_{xyn}\cos\phi_{xyn} - b_{xyn}\sin\phi_{xyn}) + j(a_{xyn}\sin\phi_{xyn} + b_{xyn}\cos\phi_{xyn}) \quad (3)$$

The phase shifted values are them summed across the array elements to form a complex image store (4).

$$A_{xy} = \frac{1}{Ne}\sum_{n=1}^{N_E} a_n \alpha'_{xyn} \quad (4)$$

The final pixel intensity (power) is given by (5).

$$I_{xy} = |A_{xy}|^2 = A_{xy}A^*_{xy} \tag{5}$$

The initial stage in the imaging process is the definition of the spatial window in terms of its type, dimensions, and the co-ordinates of its centre relative to a fixed point in space (the transmitter position). The spatial window is subdivided to provide a pixel co-ordinate map (PCM) containing the spatial point position vectors $\overline{P}_{xy}$ used to establish the imaging delays t_{xyn}. By use of a defined Cartesian co-ordinate system for delay calculation, conventional methods of matrix based co-ordinate transformation can be applied for image scaling, rotation and translation.

Imaging delays can be pre-calculated and stored in a time delay look up table (LUT) or calculated during the imaging operation with sensor position vector matrix transformations applied for image stabilisation. If $\overline{P}_{tx}$ is considered the position vector of the transmitter and $\overline{R}_n$ that of the nth receiving element, the imaging delay for the spatial point stored in the PCM at (x,y) can be expressed as

$$t_{xyn} = \frac{|\overline{P}_{xy} - \overline{P}_{tx}| + |\overline{P}_{xy} - \overline{R}_n|}{c} \tag{6}$$

where c is the local speed of sound in the medium. t_{xyn} is used to establish values of D_{xyn} and τ_{xyn}. Errors in the beamforming operation will increase proportionally with τ_{xyn} [20] and are minimised by selecting the complex spectral estimate closest to t_{xyn}.

3. SYNTHETIC APERTURE

The inherently focused nature of the DFB algorithm and method of implementation is applicable directly to establishing the imaging parameters, delays and phase correction required for synthetic aperture processing. As with forward looking imaging, there is no restriction in spatial point distribution. In order to enable continuous real time strip mapping using synthetic aperture techniques, a form of restricted processing has been applied to DFB. Coherent integration can be geometrically restricted to spatial points lying within the real aperture beamwidth, or any arbitrary portion of the real aperture pattern. The phase shifting operation can be weighted with the real aperture pattern for each PCM point which, combined with the summation in the beamforming operation forms the azimuthal matched filter. This is carried out for each point in the image scene. The operation can be subdivided into range matched filtering [21], (compression), and azimuthal matched filtering, often compared directly to conventional delay sum beamforming [9]. With reference to equation (1) the digital focused beamforming algorithm for synthetic aperture processing is as follows

$$p_{xy} = \left| \sum_{n=0}^{N} w_{xyn} s_{fn}(kT_s - D_{xyn}T_s) b_n(f_c, \theta_{xy}) \exp(-j2\pi f_c T_s \tau_{xyn}) \right|^2 \tag{7}$$

where $s_{fn}(kT_s) = e_n(kT_s) \otimes r(kT_s)$ is the correlation of the returned echo signal with a general filter function $r(kT_s)$ for a set of defined frequencies limited by the pulse bandwidth. For chirp signals, pre or post beamformer compression can be applied. For pre-beamformer compression, $r(kT_s)$ is defined by $\mathrm{rect}(t/T_p)\exp(-j2\pi[f_{\min}t + 0.5kt^2])$ or a quadrature chirp matched filter of duration T_p where f_{min} is the lower chirp frequency and k the frequency gradient. The correlation filter response envelope limits the compressed bandwidth around chirp centre f_c,[14] which is used to formulate the phase shift. Alternatively, post beamformer compression can be applied on the phase shifted complex frequency components for each image point by multiplication with the conjugate of the frequency domain representation of the transmitted pulse. Post beamformer compression increases computational load and complexity although techniques operating on a restricted number of spectral components with optimised window functions have been proposed [22]. The use of discreet frequency coded pulses enables compression to be achieved by the superposition of stepped-frequency pulse waveform segments [14].

Delay generation is adapted for the synthetic aperture geometry, as follows,

$$t_{xyn} = \frac{\left|\overline{P}_{xy} - \overline{v}t_{tx}\right| + \left|\overline{P}_{xy} - \overline{v}t_{rx}\right|}{c} \quad (8)$$

where $\overline{v}$ is the platform velocity at transmission and reception indicated by subscript. As with forward looking imaging, there is no restriction in spatial point distribution, both Cartesian and polar format SAS images can be created. Pre-calculation of imaging delays for SAS processing is feasible but results in extensive storage requirement. Equation (8) maps readily onto DSPs enabling real time delay calculation

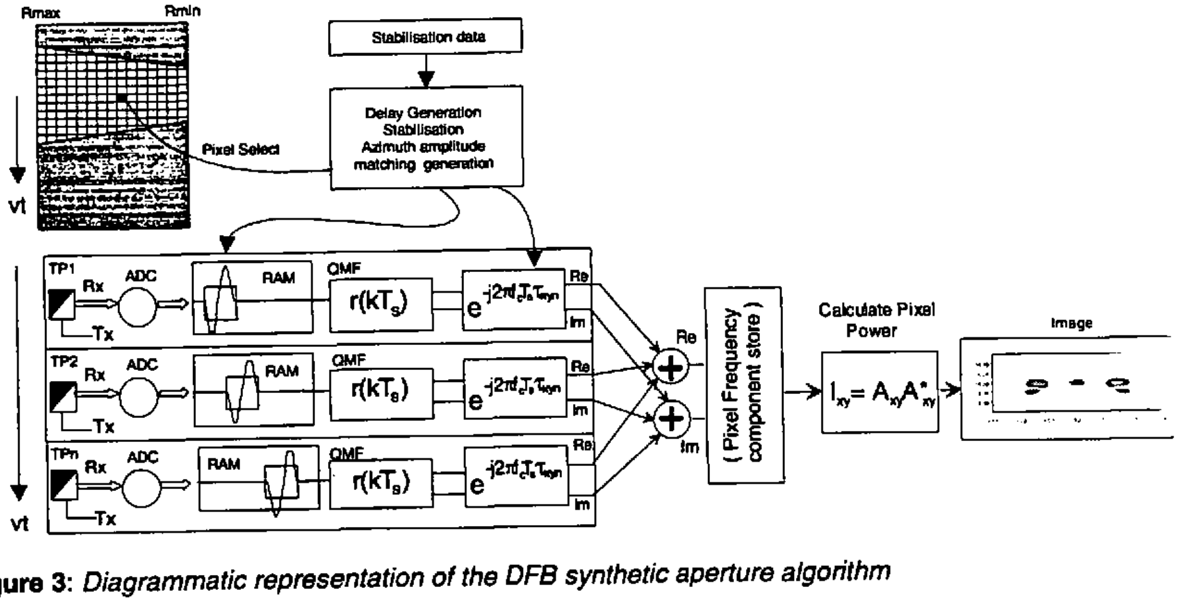

Figure 3: *Diagrammatic representation of the DFB synthetic aperture algorithm*

Various adaptations of DFB have been applied to SAS processing. The following simulations have been carried out in zero noise in order to highlight the grating lobe suppression characteristics of each processing scheme. A single point target at 10m from the centre of the defined track is used with a mid-water setting. A non-point target simulation and a real SAS image from the prototype system are presented later in the section.

Direct application of the DFB algorithm processes each successive transmission as if it were a separate array element and results in full coherent integration over the platform track. This can be considered a form of coherent averaging with phase correction, the $b_n(f_c,\theta_{xy})$ and w_{xyn} terms in (7) set to unity. Figure 4 shows the narrow band (a) and wide band (b) implementations using coherent integration over a track length of 4.76m sampled at 0.1m *(d/2)* intervals. In the wide band case the grating lobes are visibly smeared (-10dBs). Although the synthetic aperture data is inherently shaded by the real aperture response no suppression or smearing in the narrow band case is apparent.

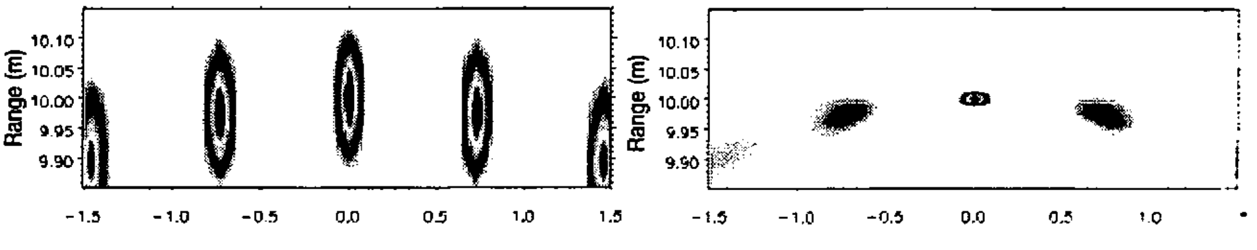

Figure 4 : *Synthetic aperture images created using full coherent integration over the platform track* **(a)** *Narrowband case using a 30 cycle 100kHz Gaussian shaded pulse showing a maximum grating lobe level of -1dB.* **(b)** *Wide band signal using a 0.3ms Gaussian weighted chirped pulse with a bandwidth of 120kHz centre at 100kHz.*

Coherent integration over all platform track positions can be combined with amplitude matching at each image point by introduction of the predicted real aperture response $b_n(f_c,\theta_{xy})$ in (7). The return from spatial points outwith the real aperture main lobe response are attenuated by the gradually decreasing sidelobe response. Figure 5 shows the narrowband and wideband cases for this processing scheme. The narrowband simulation shows a grating lobe level of -12dBs while the combined effects of smearing and aperture pattern attenuation in the wideband case reduce the grating lobes further to -19dB.

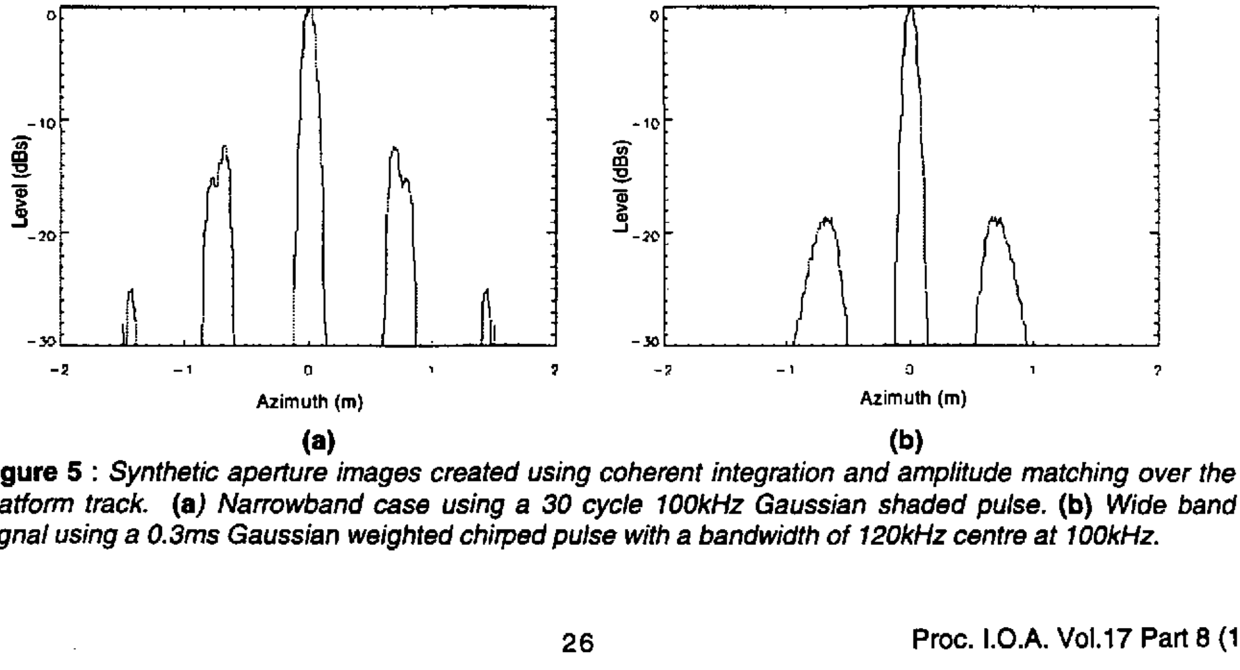

Figure 5 : *Synthetic aperture images created using coherent integration and amplitude matching over the platform track.* **(a)** *Narrowband case using a 30 cycle 100kHz Gaussian shaded pulse.* **(b)** *Wide band signal using a 0.3ms Gaussian weighted chirped pulse with a bandwidth of 120kHz centre at 100kHz.*

Each spatial point in an image will have a synthetic aperture length defined by the real aperture response at its range. Coherent integration over the individual synthetic aperture lengths can be achieved by restricting processing for a particular transmission to spatial points that lie within the real aperture main lobe response. This is achieved by defining w_{xyn} as a rectangular function based on the required synthetic aperture length at each range interval. This form of restricted spatial processing for each transmission can be applied with or without shading by the predicted real aperture response $b_n(f_c,\theta_{xy})$. The primary advantage of restricted processing is the reduction in computation load and the ability to implement real time continuous synthetic aperture swath mapping. Figure 6 shows the grating lobe suppression for the narrow band (-15dB) and wideband (-18dB) schemes without the $b_n(f_c,\theta_{xy})$ term, which is included for Figure 7 giving -17dB and -20dB lobe level for narrowband and wideband respectively.

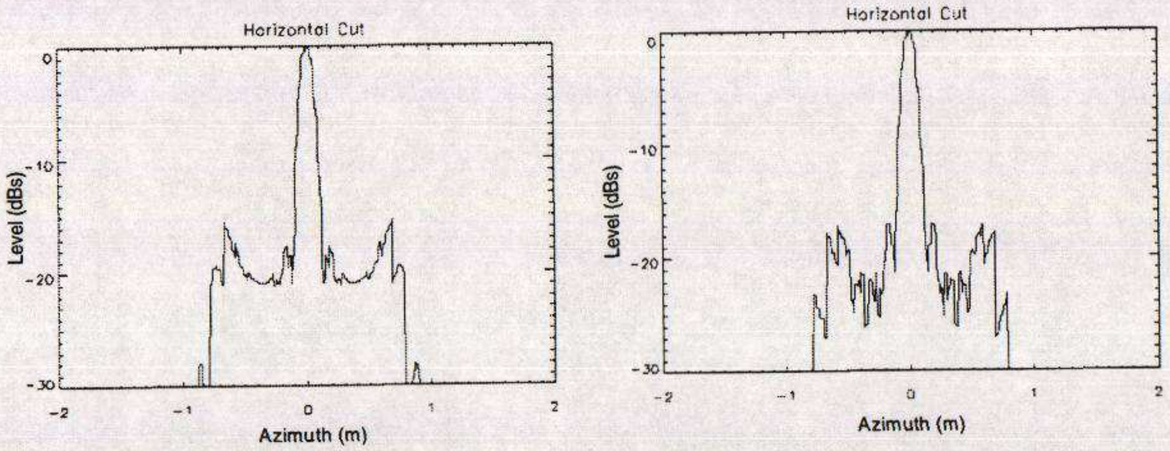

(a) (b)

Figure 6 : *Synthetic aperture images created using restricted coherent integration.* **(a)** *Narrowband case using a 30 cycle 100kHz Gaussian shaded pulse.* **(b)** *Wide band signal using a 0.3ms Gaussian weighted chirped pulse with a bandwidth of 120kHz centre at 100KHz.*

Coherent integration using restricted processing has been successfully demonstrated experimentally using the DFB prototype system. The system is designed for forward looking imaging and has been adapted for SAS processing and integrated with a 3 axis motion control system fitted to the test tank. The system is based on two TMS320C30 digital signal processors under control of a PC. Real time imaging of up to 40,000 spatial points has been demonstrated experimentally for SAS with a PRF of up to 5Hz for a continuous SAS strip mapped image. The test tank image (Figure 8a) was obtained in real time as a 4cm real aperture traversed a 3m track at a PRF of 3Hz enabling sampling at d/2.

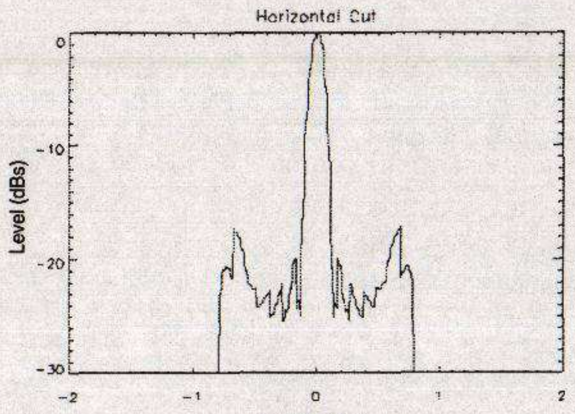

(a)

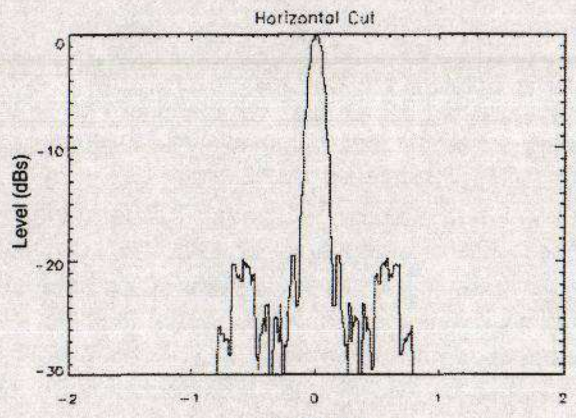

(b)

Figure 7 : *Synthetic aperture images created using restricted coherent integration and amplitude matching.* **(a)** *Narrowband case using a 30 cycle 100kHz Gaussian shaded pulse.* **(b)** *Wide band signal using a 0.3ms Gaussian weighted chirped pulse with a bandwidth of 120kHz centre at 100kHz.*

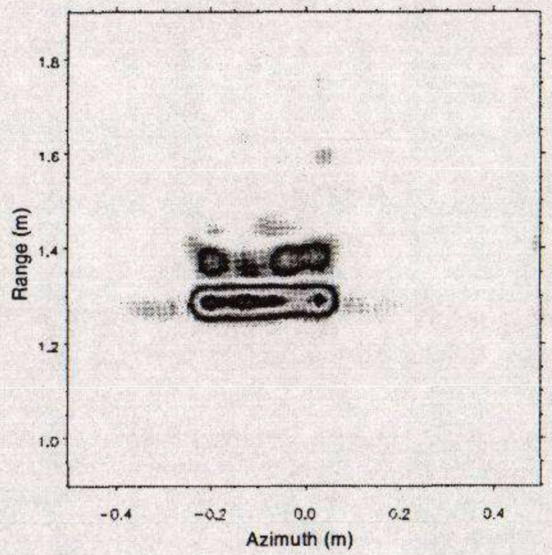

(a)

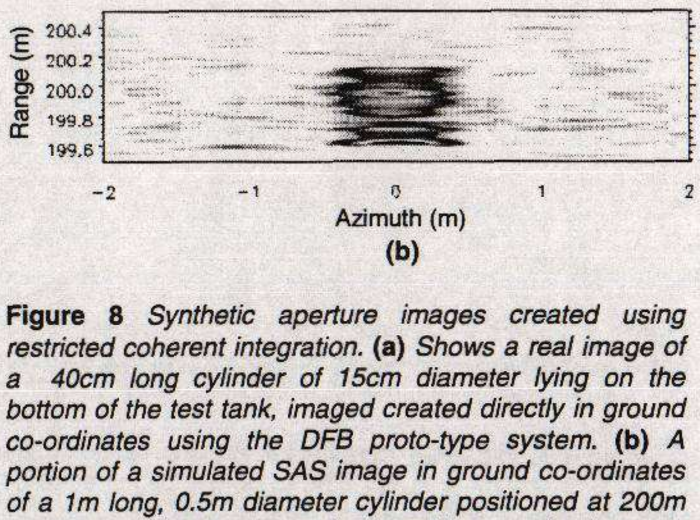

(b)

Figure 8 *Synthetic aperture images created using restricted coherent integration.* **(a)** *Shows a real image of a 40cm long cylinder of 15cm diameter lying on the bottom of the test tank, imaged created directly in ground co-ordinates using the DFB proto-type system.* **(b)** *A portion of a simulated SAS image in ground co-ordinates of a 1m long, 0.5m diameter cylinder positioned at 200m ground range at a depth of 30m with central axis along track. v = 2kt, PRF = 2.57Hz.Wideband 0.3ms pre compressed chirp pulse with 120kHz bandwidth,* f_c *=100kHz and -12dB data SNR.*

4. CONCLUSION

This paper has reviewed the application of digital focused beamforming to synthetic aperture processing. Four schemes have been assessed in their ability to suppress grating lobes. Restricting the processed pixels to those incident in the main lobe response of the real aperture has been seen to reduce the peak level of the grating lobes in the narrow band case (Figure 6a) compared with more conventional matched filter processing (Figure 5a). In the wideband case (Figure 6b) the lobes are reduced to a similar levels as Figure 5b.The noise introduced by processing however is seen to increase in presented simulations carried out in ideal conditions. The application of restricted processing also enables synthetic aperture strip mapping to be achieved without the need to collect and post process data. Significant improvements in processing throughput over the azimuthal matched filtering scheme are obtained. Combination of restricted processing and matched filtering (Figure 7) gives minor improvements in image noise and lobe level over the basic restricted processing scheme, but results in an increase in computational requirement.
DFB for forward looking imaging has inherent properties for stabilisation using matrix based transformations which can equally be applied in synthetic aperture imaging given the existence of suitable sensory data. Work is continuing in assessment of motion stability criteria associated with DFB.

The digital focused beamforming algorithm in general is considered to be versatile in its application to various modes of sonar imaging. Work is continuing in the investigation of swath bathymetry and three dimensional imaging algorithms based on DFB. Spotlight synthetic aperture processing has also been carried out both in simulation and experimentation.

5. REFERENCES

[1] IEEE Oceanic Engineering Society, *Special Issue on Acoustic Synthetic Aperture Processing*, IEEE Journal Oceanic Engineering, Vol. 17. No 1, January 1992.

[2] M P Hayes, 'A CTFM Synthetic aperture sonar', PhD Dissertation., Univ. Canterbury,Dept. Electrical and Electronic Engineering, Christchurch, New Zealand. Sept, 1989.

[3] P. de Heering, 'Alternative Schemes in Synthetic Aperture Sonar Processing', IEEE J. Ocean. Eng., Vol.9, No.4, pp277-280, Oct. 1984., [1.82]

[4] L J Cutrona, 'Comparison of sonar system performance achievable using synthetic-aperture techniques with the performance achievable by more conventional means', J. Acoust. Soc. Amer., Vol.58, No.2, pp336-348, Aug. 1975.

[5] M P Bruce, 'A processing Requirement and Resolution Capability of Side-Scan and Synthetic aperture Sonars', IEEE Journal of Oceanic Engineering, Vol 17, Number 1 (Special Issue), January 1992 pp 106-117.

[6] M P Hayes & P T Gough, 'Broad-Band Synthetic Aperture Sonar', IEEE Journal of Oceanic Engineering, Vol 17, Number 1 (Special Issue), January 1992 pp 80-94

[7] K Rolt & H Schmidt, 'Azimuthal ambiguities in Synthetic Aperture Sonar and Synthetic Aperture Radar Imagery', IEEE Journal of Oceanic Engineering, Vol. 17, Number 1 (Special Issue),January 1992 pp 74-79

[8] P. de Heering, 'Acoustic Synthetic Aperture Processing Theory and Applications', Ph.D. Dissertation, Univ. Bremen, Bremen, Germany, 1990.

[9] J Chantillon & M Zakharia, 'Navigation inaccuracies in synthetic aperture sonar: Simulations and Experimental set-up', Undersea Defence Technology (UDT 92), London, UK, June 1992, pp.553-557

[10] P T Gough & M P Hayes, 'Measurements of acoustic phase stability in Loch Linnhe', Scotland, J. Acoust. Soc. Amer., Vol.86, pp837-839, 1989.,

[11] J T Christoff, C D Loggins & E L Pipkin, 'Measurement of the temporal phase stability of the medium', J. Acoust. Soc Am., Vol. 71, pp 1606-1607, 1982
[12] R Sheriff, 'Synthetic aperture beamforming with automatic phase compensation for high frequency sonars', Proc. IEEE Symp. on Autonomous Underwater Vehicle Technology, Washington DC, June 1992. PP.236-45.
[13] Raven, R.S., 'Electronic Stabilisation for displace phase center systems', US Patent 4244036, January 1981.
[14] D R Wehner, 'High Resolution Radar',Artecth House Inc, 1987.
[15] R McHugh,S Shaw & N Taylor, 'A general purpose digital focused beamformer', Proc. Oceans '94, Vol. 1, pp 229-234, Brest, France, Sept. 1994.
[16] R A Mucci, 'A Comparison of Efficient Beamforming Algorithms', IEEE Trans. ASSP, Vol.32, No.3,pp548-558, June 1984.
[17] R W Schafer, 'A Digital Signal Processing Approach to Interpolation', Proc. IEEE, Vol.61, No.6, pp692-702, June 1973.
[18] S Ries, 'High Frequency Digital Time-Delay Beamforming for Demodulated Bandpass Signals', Proc. IoA, Vol.13, Pt.9, pp268-275, 1991.
[19] R G Pridham & R A Mucci, 'Digital Interpolation Beamforming for Low-Pass and Bandpass Signals', Proc. of IEEE, Vol.67, pp904-919, June 1979.
[20] J G Paul, 'Simulation and Analysis of a Digital Focused Beamformer for Sonar', PhD thesis, Department of Electrical and Electronic Engineering, Heriot-Watt University, Edinburgh, June 1992.
[21] J P Fitch, 'Synthetic Aperture Radar', Springer-Verlag,1988.
[22] G Shippey & R McHugh, 'Efficient time domain acoustic imaging with a wideband source', Proceeding of 2nd European Conference on Underwater Acoustics, Vol. 2, pp 709-714, July 1994.

ACKNOWLEDGEMENT

This work is funded by the Marine Technology Directorate (MTD) agent of the Engineering and Physical Science Research Council (EPSRC) and by the Defence Research Agency (DRA) Maritime Division. We would like to thank J Wickenden and Sean Chapman of DRA Bincleaves for their continuing support and encouragement during the course of this work.